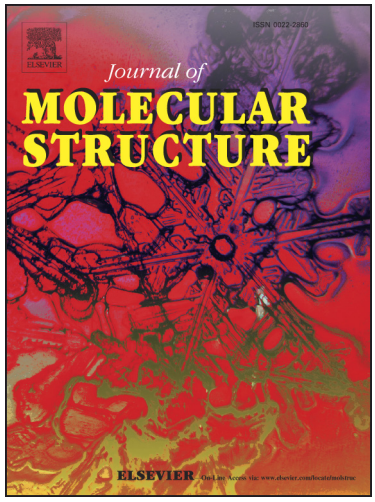

Synthesis, spectroscopic characterization of novel 16α-(3-acetyl phenyl amino)-3β- hydroxy pregn-5-ene-20-one, its molecular structure, NBO analysis, intramolecular interactions studied by DFT and AIM approach

Arun Sethi, Dolly Shukla, Ranvijay Pratap Singh

PII: S0022-2860(14)00582-1
DOI: http://dx.doi.org/10.1016/j.molstruc.2014.05.068
Reference: MOLSTR 20667

To appear in: *Journal of Molecular Structure*

Received Date: 25 March 2014
Revised Date: 26 May 2014
Accepted Date: 26 May 2014

Please cite this article as: A. Sethi, D. Shukla, R.P. Singh, Synthesis, spectroscopic characterization of novel 16α-(3-acetyl phenyl amino)-3β- hydroxy pregn-5-ene-20-one, its molecular structure, NBO analysis, intramolecular interactions studied by DFT and AIM approach, *Journal of Molecular Structure* (2014), doi: http://dx.doi.org/10.1016/j.molstruc.2014.05.068

Synthesis, spectroscopic characterization of novel 16α-(3-acetyl phenyl amino)-3β- hydroxy pregn-5-ene-20-one, its molecular structure, NBO analysis, intramolecular interactions studied by DFT and AIM approach

Arun Sethi[a]*, Dolly Shukla[a] and Ranvijay Pratap Singh[a]

[a]*Department of Chemistry, University of Lucknow, Lucknow 226007, India*

ABSTRACT:

A novel compound 16α-(3-acetyl phenyl amino)-3β- hydroxy pregn-5-ene-20-one was **s**ynthesized by Michael addition reaction and characterized with the aid of ^{1}H, ^{13}C-NMR, IR, UV and Mass spectrometry. The molecular geometry of synthesized compound was calculated in the ground state by density functional theory (DFT/B3LYP) using 6-31G (d, p) basis set. ^{1}H and ^{13}C-NMR chemical shifts were calculated using Gauge-Including Atomic Orbital (GIAO) approach and these values were correlated with the experimental observations. The electronic properties such as HOMO and LUMO energies were calculated using time dependent density functional theory (TD-DFT). Stability of the molecule as a result of hyperconjugative interactions and electron delocalization were analyzed using natural bond orbital (NBO) analysis. Intramolecular interactions were analyzed by AIM approach. Local reactivity descriptors were calculated to study the reactive site within the molecule.

Keywords: Pregnane, Michael addition, β-amino ketones, TD-DFT, NBO, AIM approach.

* Corresponding author. Tel: +919415396239

E-mail addresses: alkaarunsethi@rediffmail.com(A.Sethi)

1. Introduction

β-amino ketones are useful synthons for the synthesis of nitrogen containing bioactive molecules [1]. Important biological activities like antibacterial, antiviral, analgesic and antitumor properties have been reported to be associated with molecules having nitrogen and sulfur atoms individually or in combination [2-9]. Pregnenolone and its derivatives have been reported to possess anti-inflammatory, anti-asthmatic, cytotoxic, anti-feedant, anti-dyslipidimic, anti-oxidant and anti-viral properties [10-16]. Taking this into account, we planned to synthesize a novel *β*-amino ketone derivative of pregnane by adopting Michael addition reaction [15, 17] **scheme 1**.

The structure of synthesized compound **3** was interpreted with the help of ^{1}H, ^{13}C NMR, IR, UV-Visible spectroscopy and mass spectrometry. Geometry of compounds **1** and **3** were optimized and vibrational frequencies of compound **3** was calculated using density functional theory (DFT) with the help of B3LYP functional and 6-31 G (d,p) basis set. The results were compared with the experimental observations. Further, nuclear magnetic chemical shifts were calculated with the same functional and basis set using GIAO method and results were compared with the experimental data. HOMO-LUMO analysis was also carried out to predict various transitions using time dependent TD-DFT approach. AIM approach has extensively been applied to classify and understand hydrogen bonding interactions and ellipticity in the synthesized molecule. Local reactivity descriptors were calculated to study the reactive site within the molecule.

2. Experimental

2.1. Materials and Methods

All solvents used were of analytical grade and were purified and dried according to standard procedures (A.I. Vogel, Practical Organic Chemistry) prior to their use. Thin layer chromatography (TLC) was performed on Silica Gel 'G' (Merck, India) coated plates for monitoring the progress of reaction. ^{1}H nuclear magnetic resonance (NMR) was recorded on Bruker DRX–300 MHz and ^{13}C NMR was recorded on JOEL AL 300 FTNMR (75Mz) using TMS as an internal reference. IR spectra were recorded on Perkin Elmer FTIR spectrometer from 4000–450 cm^{-1} range. The spectra were analyzed using Spectrum™ Software suite. The spectra were measured with 4 cm^{-1} resolution and 1 scan co-addition. ESI–MS spectra were recorded on Agilent 6520 Q–TOF mass spectrometer. Ultraviolet absorption spectra were obtained (in the range of 200-450 nm) using ELICO BL-200 UV-Vis spectrophotometer equipped with a 10 mm quartz cell in chloroform.

2.2. Synthesis of 16α-(3-acetyl phenyl amino)-3β- hydroxy pregn-5-ene-20-one

200 mg (0.636 mmol) of 3β- hydroxy pregn-5, 16-diene-20-one was dissolved in 20 mL of freshly distilled dry acetonitrile followed by addition of 85.97 mg (0.636 mmol) of *m*-amino acetophenone. The reaction mixture was refluxed for 18 hours. Ice cold solution of sodium bicarbonate was added to the reaction mixture. The synthesized compound was extracted with

chloroform (3 x 15mL) and the combined organic extract was washed with water, dried over anhydrous sodium sulphate. The organic layer was concentrated under reduced pressure and the crude concentrated product was purified by column- chromatography using ethyl acetate: hexane (15: 85) affording 16α-(3-acetyl phenyl amino)-3β- hydroxy pregn-5-ene-20-one as viscous. Molecular formula: $C_{29}H_{39}NO_3$. ^{1}H NMR (300 MHz,$CDCl_3$) δ (ppm): 7.03 (1H,t, H-68**,** J=7.8Hz), 6.64(1H,d, H-67, J=6.3 Hz.), 6.56 (1H,s, H-63), 6.42 (1H, d,H-69, J=6.3Hz.),5.32 (1H,d, H-42, J=5.1 Hz), 4.41 (1H,t, H-57,J=7.5), 3.56-3.47(1H,m, H-38), 4.26 (bs, 1H, -NH), 2.44 (1H,d, H-58) 2.26 (3H,s, H-64,65,66), 2.16(3H,s, H -59,60,61) 1.01 (3H,s, H- 70,71,72), 0.72 (3H,s, H-51,52,53). ^{13}C NMR (75 MHz, $CDCl_3$) δ (ppm): 211.91 (C=O, C-20), 198.27 (C=O, C-29), 148.67 (C-23**),** 140.72 (C-5), 135.35(C-25), 130.55 (C-27), 121.48 (C-6), 117.27 (C-28), 113.06(C-26), 111.28 (C-24), 71.77(C-3), 69.30(C-17), 54.88(C-14), 49.90(C-9), 49.33(C-4), 45.45(C-16), 42.33(C-2), 37.29(C-1), 36.63(C-13), 35.69(C-10), 35.12(C-12), 32.82(C-7), 32.10(C-15), 31.73(C-30 &C-8), 29.90(C-21), 21.47 (C-19), 20.82 (C-11), 19.56(C-18). ESI–MS: m/z = [M^+ + Na] 472,442,422,313,274. IR νmax (in cm^{-1}): 3384.5, 2928.10, 2852.90, 1700.21, 1660.91, 1594.01, 1489.25, 1450.79, 1354.48, 1317.59, 1292.67, 1255.91, 1071.89, 814.36, 754.97, 665.88, 500.46.

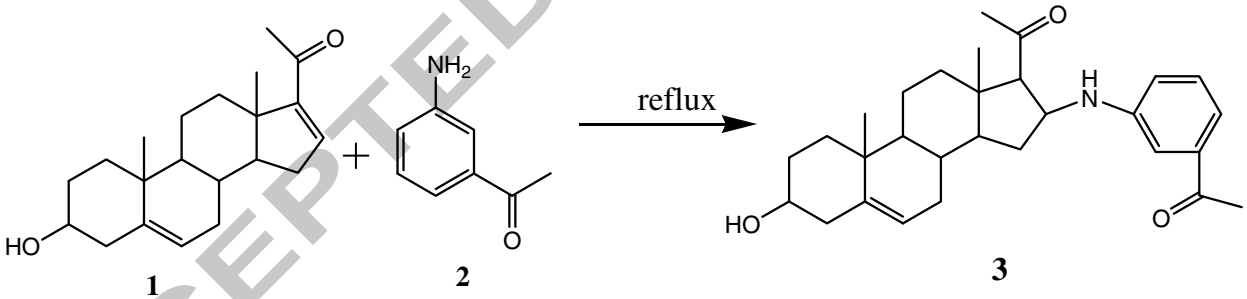

Scheme 1

2.3. Computational study

The molecular geometry optimization for compound **3** was carried out with Gaussian 03 program package [18] using B3LYP functional with the 6-31G (d, p) basis set. The ^{1}H and ^{13}C-NMR isotropic shielding of **3** was calculated with the help of GIAO method [19] using B3LYP/ 6-31G (d, p) basis set. UV-Vis spectra, electronic transitions and electronic properties such as HOMO-LUMO were computed with the help of time-dependant DFT (TD-DFT) method. Stability of the

molecules as a result of hyperconjugative interactions and electron delocalization were analyzed using Natural Bond Orbital (NBO) analysis [20]. Presentation graphics including visualization of the molecular structures were done with the help of Gauss View [21] and intramolecular interactions analyzed by AIM approach [22].

3. RESULT AND DISCUSSION

3.1. Molecular structure

Optimized geometrical parameters of compounds **1** and **3** presented in **Fig 1** and **Fig 2** were calculated at B3LYP/6-31G (d, p) and comparison between the two optimized structures were also carried out and presented in **Table 1**. The introduction of $-NH_2$ group of *meta*-amino acetophenone at C-16 position in compound **1** showed increase in C16-C17 bond length, thereby confirming the conversion of double bond (1.34 Å) to single bond (1.57 Å) in compound **3**. Bond length obtained from theoretical observations of N-C23 was found to be 1.38Å, which is almost similar to N-C bond length ~ 1.35 Å in aromatic amine while bond length between C16-N was found to be 1.45Å which is also nearly similar to C-N bond length ~1.46 Å in aliphatic amine.

Torsional angle between C_{13}-C_{17}-C_{20}-O(C=O) in compound **1** was -178.39^o whereas in compound **3**, this angle was found to be -83.51^o. The change in torsional angle appears to be due to rotation of carbonyl group, which is in plane with the five member ring in compound **1,** while in compound **3**, it is inclined below the plane, and this may probably be due to introduction of *m*-amino acetophenone at C-16. Bond angle between C_{15}-C_{16}-C-$_{17}$ (112.58^o) of compound **1** was greater in comparison with that of compound **3** (105.49^o) and this is due change in the hybridization of C-16 and C17 carbons. In compound **1** the C-16 and C17 carbons were sp^2 hybridized, whereas in compound **3** they were sp^3 hybridized. The deviation of bond angle from the normal 120^o angle (sp^2 hybridized) in case of compound **1** appears to be because C-16, C-17 double bond is in conjugation with the carbonyl group at C-20 position. Whereas in compound **3**, the deviation from the normal tetrahedral angle appears to be due to bond pair- lone pair repulsion (lone pair of nitrogen of amino group and bond pair of C_{15}-C_{16} or C_{16}-C-$_{17}$), which resulted in the decrease in the bond angle.

3.2. ^{1}H and ^{13}C-NMR Spectroscopy

The ^{1}H and ^{13}C NMR chemical shift of compound **3** were calculated with gauge-including atomic orbital (GIAO) approach using B3LYP/6-31G (d, p) basis set. The experimental and calculated values of ^{1}H and ^{13}C NMR chemical shifts of the newly synthesized compound **3** are given in **Table 2**. The correlation between the experimental and calculated ^{1}H NMR chemical shift values of these compounds are plotted in graph **Fig 3**. These graphs shows good correlation between the experimental and the calculated results with the coefficient of regression (R^2) being in the range of 0.99013 The experimental and calculated values of ^{13}C-NMR chemical shifts of the newly synthesized compound **3** are given in **Fig 4**. The graphs shows good correlation between the experimental and the calculated results with the coefficient of regression (R^2) being in the range of 0.99241.

The ^{1}H NMR spectrum (**fig 5**) of compound **3** showed, one proton triplet at δ 4.41 (J= 7.5 Hz) for H-57 proton, one proton triplet at δ 7.03 (J= 7.8 Hz) for H-68, one proton doublet at δ 6.64 (J= 6.3 Hz) for H-67, one proton singlet at δ 6.56 for H-63 and one proton doublet at δ 6.42 (J= 6.3 Hz) for H-69. The appearance of these four aromatic proton, along with the broad singlet for the secondary amino proton at δ 4.26 as well as the position of H-57 proton in spectrum showed that the bonding has taken place between the C-16 carbon of the pregnane and amino group of *m*-amino acetophenone and not between C-16 carbon of the pregnane and carbon of the aromatic ring. Besides this, some other characteristics peaks for pregnane moiety were also observed in the ^{1}H NMR spectrum. The H-42 and H-58 proton were observed as a doublet at δ 5.32 (J= 5.1 Hz) and 2.44 (J= 6.0 Hz) respectively and four singlets of three protons each δ2.26, 2.16, 1.01, and 0.72 due to methyl groups at C-30 (H-64,65,66), C-21(H -59,60,61), C-19(H-70,71,72) and C-18(H-51,52,53) respectively.

The ^{13}C NMR spectrum of compound **3** in **Fig 6** showed that the signal for C-16 carbon, which is directly bonded to -NH_2 group was observed at δ45.45 (if this carbon was bonded with the carbon of the aromatic ring then signal for C-16 carbon would be observed upfield), This together with signals for carbons of the aromatic ring at δ 148.67, 135.35, 130.55, 117.27, 113.06, 111.28 for C-23, C-25, C-27, C-28 (if C-28carbon was bonded with the carbon of C-16 of the pregnane then the signal for C-28 would be observed downfield but in compound **3** bonding has taken place between nitrogen atom of amino group and carbon of C-16, due to this

the signal for C-28 carbon was observed at δ 117.27), C-26, C-24 respectively and a signal for carbonyl group at 198.27 (C-29) confirmed the introduction of *m*-amino acetophenone at C-16 position through the nitrogen atom of amino group. Besides this all the signals for pregnane moiety were also observed. The carbonyl carbon present at C-20 position was observed at δ 211.91. Olefinic carbons at C-5, C-6 positions were found to be at δ 140.72 and 121.48 respectively. Carbon at C-3 position was observed at δ 71.77, downfield shifting of it is due to presence of hydroxyl group. Three methyl signals of pregnane were observed at δ 29.90, 21.47 and 19.56 which are due to C-21, C-19 and C-18 carbons respectively.

3.3. UV-Visible Spectroscopy

The UV-Visible spectrum of compound **3** has been studied by time dependent density functional theory (TD-DFT). The HOMO-LUMO energy gap of compound **3** has been calculated at B3LYP/6-31G (d, p) basis set. The energy gap between the HOMO and LUMO is a critical parameter in determining molecular electrical transport properties because it is a measure of electron conductivity [23].The absorption wavelengths for compound **3** presented in **Table 3** were observed at 356 nm, 304 nm and 256 nm. The experimental band at 356 nm is attributed to H→L transition and the band observed at 304 nm is due to H→L+1 while the band at 256 nm is attributed to H→L+2 transitions. The transitions in compound **3** were predicted to be due to n→ π* and π→ π* transitions. UV spectrum of compound **3** is given in **Fig. 7** and orbital picture of molecular orbitals is shown in **fig 8.**

3.4. NBO analysis

NBO analysis has an appealing aspect of highlighting the individual bonds and lone–pair energy that play a vital role in the chemical processes [24-26]. It is an important tool for studying hybridization, covalence, hydrogen–bonding and Vander Waals interactions. In other words Natural Bond Orbital (NBO) provides supplementary structural information. Second–order perturbation theory analysis of the Fock matrix in NBO basis for compounds **3** is presented in **Table 4.** The higher value of E (2) (stabilization energy or energy of hyper conjugative interaction) points towards the greater interaction between electron donors and electron acceptors (i.e. the more donating tendency from electron donors to electron acceptors and the greater the extent of conjugation in the system). Delocalization of electron density between occupied Lewis-

type (bonding or lone pair) NBO's and unoccupied (antibonding) non-Lewis NBO's correspond to a stabilizing donor–acceptor interaction. In compound **3** some of the important π→π* interactions viz. π (C23–C24) → π*(C28–C27)/ π*(C24–C25); π(C28–C27)→ π*(C23–C24)/ π*(C26–C25); π (C25–C26)→ π*(C23–C24)/ π*(C28–C27)/ π*(C29–O31) are responsible for the delocalization of respective π–electrons of acetophenone ring, the molecule being stabilized by energy in the region of 17.51~23.06 kJ/mol. Other high energy interactions involving the lone pair of electrons with the anti-bonding π electrons corresponds to n_2 (O32) → π*(C20–C17), n_2 (O31) → π*(C25–C29) and n_2 (O31) → π *(C29–C30) stabilizing the molecule with 19.45 kJ/mol, 19.45 kJ/mol and 20.12 kJ/mol respectively and n_1 (N22) →π*(C23–C24) interaction indicates the delocalization of lone pair of electrons on the nitrogen atom of -NH group with anti-bonding π–electron in acetophenone ring with maximum stabilization energy in the region of 34.27 KJ/mol.

3.5. Vibrational Assignment

The Calculated and Experimental IR spectrum of compound **3** were found in the region 450-4000 cm^{-1} presented in **Table 5**. The calculated vibrational wavenumbers are higher than the experimental wavenumbers due to discard of anharmonicity present in real system. Therefore, calculated wavenumbers are scaled down by a single factor 0.9608 to compare with experimental wavenumbers. The scaled vibrational wavenumbers helps in the assignment of vibrational modes obtained from experimental FT-IR spectrum. The correlation graphs of the experimental and calculated wave numbers were compared. The value of correlation co-efficient (R^2= 0.9995) shows good agreement between experimental and calculated wave numbers. The correlation graph is presented in **Fig 9**.

3.5.1. C-N and N-H vibrations

In IR spectrum (**Fig 10)** of compound **3,** two bands for C-N stretching vibration were observed, one between aromatic carbon and nitrogen and second between aliphatic carbon and nitrogen. Stretching vibration for N22-C23 was observed at 1317.59 cm^{-1}, showing good agreement with the calculated wave number at 1304 cm^{-1}. Stretching vibration for C16-N22 observed at 1255.91cm^{-1}, shows good agreement for calculated wave number at 1213 cm^{-1} [27]. Besides, two wave number for C-N stretching vibration, N-H stretching vibration for secondary amine was

also observed at 3384.33 cm^{-1} shows that *meta*-amino acetophenone on introduction in compound **1** become secondary aromatic amine in compound **3.** Besides this N-H bending vibration for secondary amine and N-H wagging vibration were observed at 1489.25 and 814.36 cm^{-1} showing good agreement with the calculated wave number at 1493 $cm^{-1}$and 844.9 cm^{-1} respectively.

3.5.2. C=C vibrations

The C=C stretching vibration of olefin was observed at 1660.91 cm^{-1}. The calculated wave number at 1674 cm^{-1} assigned to the C=C stretching vibration mode of olefin present at C5-C6. In aromatic hydrocarbon, experimental values of C=C ring stretching observed at 1594, 1450.79 cm^{-1}[28-29] were found to be in good agreement with the calculated values at 1590 and 1402cm^{-1} respectively.

3.5.3. C-H vibrations

Four methyl groups are present in the molecule, out of four two methyl group present at angular position and third is attached to the C=O of ketone, while fourth is attached to the C=O of aromatic ketone. They are assigned as Me-18, Me-19, Me-21 and Me-30. The observe stretching vibration for methyl group at 2928.10 cm^{-1} for Me-21 shows good agreement with the calculated wave numbers at 2987 cm^{-1} for Me-21. The CH_2 stretching vibration observed at 2852.90 cm^{-1} shows good agreement with the calculated wave number at 2864 cm^{-1}. Asymmetric deformation of Me-30 was observed at 1354 cm^{-1}, whereas the calculated value was found to be 1339 cm^{-1}. The observed band at 1292.67 cm^{-1} was assigned to CH_2 wagging and twisting corresponds to the calculated wave number at 1289cm^{-1}. The observed band at 754.97 and 665.88 cm^{-1} assigned to aromatic C=C-H out of plane bending corresponds to the calculated wave number at 761.2 and 676.7cm^{-1}.

3.5.4. C=O and C-O vibrations

In the molecule carbonyl groups (C=O) are present at C-20 and C-29, but in IR spectrum only one band observed at 1700 cm^{-1}[28-29]. The calculated wave number for C=O group at C-20 and C=O group at C-29 showed vibrations at 1716 and 1705 cm^{-1} respectively. The observed at 1071.89 cm^{-1} assigned as C-O(C3-O39) corresponds to the calculated wave number at 1052 cm^{-1}.

4. Mass spectrometry

The structure of compound **3** was further confirmed by mass spectrometry presented in **Fig. 11**. Though M^+ of the compound at m/z 449 was not observed, however [M^+ + Na] was observed at m/z 472. Other fragments observed are m/z 442 [M^+ + Na – $2CH_3$], m/z 422 [M^+ + Na – $2CH_3$ – H_2O – 2H], m/z 313 [M^+– C_8H_9NO-H^-], m/z 274[M^+ + Na-CH_3CO-CH_2=C=O-C_2H_2-$2C_2H_4$-CH_3^+].

5. AIM approach

Geometrical as well as topological parameters are useful tool to characterize the strength of hydrogen bond. The geometrical criteria for the existence of hydrogen bond are as follows: (i) the distance between proton (H) and acceptor (A) should be less than the sum of the Van der Waal's radii of these atoms. (ii) The angle between 'donor (D), proton (H) and acceptor (A)' should be greater than 90°. (iii) There should be elongation of 'donor (D) proton (H)' bond length. As the above criteria were often considered insufficient, hence the existence of hydrogen bond was supported further by Koch and Popelier criteria [30] based on 'Atoms in Molecules' theory (i) the existence of bond critical point for the 'proton (H) . . . acceptor (A)' contact as a confirmation of the existence of hydrogen bonding interaction. (ii) The value of electron density (ρH. . .A) should be within the range 0.002–0.040 a.u. (iii) The corresponding Laplacian $^2\rho_{(r_{BCP})}$ should be within the range 0.024–0.139 a.u. According to Rozas et al. [31] the interactions may be classified as follows: (i) strong H-bonds are characterized by $\nabla^2\rho_{(BCP)} < 0$ and $H_{BCP} < 0$ and their covalent character is established. (ii) Medium H-bonds are characterized by $\nabla^2\rho_{(BCP)} > 0$ and $H_{BCP} < 0$ and their partially covalent character is established. (iii) Weak H-bonds are characterized by $\nabla^2\rho_{(BCP)} > 0$ and $H_{BCP} > 0$ and they are mainly electrostatic (where, $\nabla^2\rho_{(BCP)}$ and H_{BCP} are Laplacian of electron density and total electron energy density at bond critical point respectively).The weak interactions are characterized by $\nabla^2\rho_{(BCP)} > 0$ and $H_{BCP} > 0$ and the distance between interacting atoms is greater than the sum of Van der Waal's radii of these atoms. Molecular graph of the compound **3** using AIM program at B3LYP/6- 31G (d,p) level is presented in **Fig.12.** Geometrical as well as topological parameters for bonds of interacting atoms are given in **Table 6,** and on the basis of above criteria, as all $\nabla^2\rho_{(BCP)}$ and H_{BCP} parameters were greater than zero, hence H_{70}…H_{47}, H_{34}…H_{48}, $H_{72...}H_{45}$, H_{45}…H_{51}, H_{50}…H_{60},

$H_{57}…H_{69}$, $O_{32}…H_{69,}$ are weak interactions. In this article, the Bader's theory application was used to estimate hydrogen bond energy (*E*). Espinosa proposed proportionality between hydrogen bond energy (*E*) and potential energy density (V_{BCP}): $E = 1/2(V_{BCP})$ [32]. According to AIM calculation, the total energy of intramolecular interactions was calculated as -8.74 kcal/mol. The ellipticity (ε) at BCP is a sensitive index to monitor the π-character of bond. The ε is related to λ_1 and λ_2, which correspond to the eigen values of Hessian and defined by a relationship: $\varepsilon = (\lambda_1/\lambda_2) - 1$. The ellipticity values for bonds C23-C24, C24-C25, C25-C26, C26-C27, C27-C28, and C28-C23 were 0.216, 0.211, 0.197, 0.222, 0.223, and 0.211 respectively. The lower values of ellipticity confirm that there is delocalization of electron in aromatic ring [33]. However the higher ellipticity value for C5-C6 bond (0.372) shows electrons of this bond are not delocalized.

6. Reactivity descriptors

Local reactivity descriptors such as local softness (S_k), Fukui Function (FF) and local electrophilicity index (ω_k) [34, 35] have been used in DFT theory of chemical reactivity for defining the reactive site within a particular molecule. Fukui function *f*(r) is considered as one of the most fundamental indicator for defining the site selectivity in a given molecular species and for soft-soft type of interactions, the preferred reactive site in a molecule is the one with maximum values of ($f_{k,}$ $s_{k,}$ ω_k) [36]. Using Hirshfeld atomic charges of neutral, cation and anion state of initial compound **1** and **3**, the condensed Fukui functions (f_k^+, f_k^-, f_k^0), local softness (s_k^+, s_k^-, s_k^0) and local electrophilicity indices (ω_k^+, ω_k^-, ω_k^0) for atomic sites C-16 and C-17 were calculated and are listed in **Table 7**. In case of compound **1** the values of f_k^+, s_k^+, ω_k^+ for two atomic sites C-16 and C-17 are 0.1831, 0.0361, 0.5177 and 0.0712, 0.0140, 0.2013 respectively. Similarly for compound **3**, the values of local reactivity descriptors f_k^+, s_k^+, ω_k^+ for atomic sites C-16 and C-17 are 0.0082, 0.0016, 0.0253 and 0.0099, 0.0019, 0.0303 respectively. Maximum values of all the three local reactivity descriptors (f_k^+, s_k^+, ω_k^+) in case of compound **1** indicate that C-16 site is more prone for nucleophilic attack in comparison to C-17 atomic site. Therefore, these local reactivity descriptors calculated in case of compound **1**, confirms the favorable site of attack at C-16 position which further leads to the formation of the compound **3**.

6. Conclusion

A novel compound **3 s**ynthesized in one step by adopting Michael addition reaction has been characterized with the help of ^{1}H, ^{13}C-NMR, IR, UV and Mass spectrometry. Compound **3** was optimized by density functional theory (DFT) with B3LYP/6-31G basis set.^{1}H and ^{13}C-NMR chemical shift were calculated with the help of gauge-including atomic orbital (GIAO) approach showing good agreement with experimental chemical shift. The UV-Visible spectrum of compound has been studied by time dependent density functional theory (TD-DFT) showing n→ π* and π→ π* transition in compound **3**. Natural bond orbital (NBO) analysis showing π→ π*, σ → σ * and n→ π* hyper conjugative interactions and electron delocalization, point to the stabilization of the molecule. Intramolecular hydrogen interaction and ellipticity studied by AIM approach showed weak hydrogen interactions and π-character of bond in aromatic ring. The local reactivity descriptors calculated in case of compound **1**, confirms the favorable site of attack at C-16 position which further leads to the formation of the compound **3**.

Acknowledgement

The authors are grateful to the SAIF division of the Central Drug Research Institute, Lucknow, and IIT Kanpur for providing spectroscopic data.

References

[1] Liu, M.; Sibi. M.P. Tetrahedron. 2000, 58, 7991-8030

[2] Lalezari, I.; Shafiee, A.; Yazdani, S. J. Pharm. Sci. 1974, 63, 628-631 and references cited therein.

[3] Reddy, D. B.; Padmaja, A.; Reddy, M. M. J. Ecotox. Environ. Monit.1993, 3, 87-90.

[4] Shafiee, A.; Lalezari, I.; Yazdani, S.; Pournorouz, A. J. Pharm. Sci. 1973, 62, 839-842.

[5] Chopleo, C.V.; Mayers, P.L.; Smith, A.C.B.; Stilling, M.R.; Tulloch, I.F.; Walter, D.S. J. Med. Chem. 1988, 31, 7-13.

[6] Clemence, F.; Joliveau-Maushart, C.; Meirer, J.; Cered, J.; Cered, F.; Benzoni, J.; Deraedt, R. Eur. J. Med. Chem. Chim. Ther. 1985, 20, 257-260.

[7] Gadad, A.K.; Mahajanshetti, C.S.; Nimbalkar, S.; Raichurkar; A. Eur. J. Med. Chem. 2000, 35, 853-857.

[8] Miyahara, M.; Nakadata, M.; Sueyoshi, S.; Tanno, M.; Kamio, S. Chem. Pharm. Bull. 1982, 30, 4402-4408.

[9] Thomas, E.W.; Nishizawa, E.E.; Zimmermann, D.D.; Williams, C.J. J. Med. Chem. 1985, 28, 442-447.

[10] Nobile, A.; Charney, A. W.; Perlman, P. L.; Herzog, H. L.; Paynee, C. C.; Tully, M. E.; Jevnik, M. A.; Hershberg, E. B. J. Am. Chem. Soc. 1955, 77, 4184

[11] Zhangqing, Y.; Khalil, M. A.; Doon Hoon, K.; Lee, H. J. Tetrahedron Lett. 1995, 36, 3303;

[12] Shen, Y.; Burgoyne, D. L. J. Org. Chem. 2002, 67, 3908.

[13] Schun, Y.; Cordell, G. A. J. Nat. Prod. 1987, 50, 195.

[14] Purushothaman, K. K.; Sarada, A.; Saraswathi, A. Can. J. Chem. 1987, 65, 150.

[15] Arun Sethi, Atul Maurya, Vibha Tewari, Sanjay Srivastava, Shaheen Faridi, Gitika Bhatia, M. M. Khan, A. K. Khanna and J. K. Saxena Bioorganic & Medicinal Chemistry 15 (2007) 4520–4527

[16] Comin, M. J.; Maria, M. S.; Roccatagliate, A. J.; Pujal, C. A.; Damonate, E. B. Steroids 1999, 64, 335

[17] Arun Sethi, Gitika Bhatia, Ashok K. Khanna, Mohammad Mobin Khan, Abha Bishnoi, Anil K. Pandey, Atul Maurya., Med Chem Res (2011) 20:36–46

[18] M.J. Frisch.et.al, Gaussian 03, Revision C.02, Gaussian Inc., Wallingford, CT, 2004.

[19] K. Wolinski, J. F. Hinton, P. Pulay, J. Am. Chem. Soc., 112 (1990)8251–8260

[20] M. Sarafran, A. Komasa, E. B. Adamska, J. Mol. Struct., 827 (2007) 101–107

[21] Computer program Gauss View 3.09, Ver. 2, Gaussian, Inc., PA. Pittsburgh

[22] R.F.W.Bader, J.R.Cheeseman.AIMPAC, 2000

[23] J. Fleming, Frontier Orbitals and Organic Chemical Reactions, 249 S, Wiley, London, 1976

[24] V. Pophristic, L. Goodman, N. Guchhait, J. Phy. Chem., 101 (1997) 4290–4297

[25] D. Geo, L. Goodman, J. Phys. Chem., 100 (1996) 12540–12545

[26] F. Weinhold, Nature, 411 (2001)539–541

[27] Maryam Hatamzadeh, Ali Mahyar, Mehdi Jaymand., *J. Braz. Chem. Soc.*, Vol. 23, No. 6, 1008-1017, 2012.

[28] R. M. Silverstein, F. X. Webster, Spectrometric Identification of Organic Compounds 6th Edition, Jon Willey Sons Inc, New York, 1963.

[29] Arun Sethi, Akriti Bhatia, Atul Maurya, Anil Panday, Gitika Bhatia, Atul Shrivastava, Ranvijay Pratap Singh, Rohit Prakash, Journal of Molecular Structure, 1052(2013)112-124

[30] U.Koch, P. Popelier, J.Phys.Chem.A 99(1995)

[31] I. Rozas, I.Alkorta, J.Elguero, J.Am.Chem.Soc.122 (2000) 11154-11161

[32] E.Espinosa, E.Molins, C.Lecomte, Chem.Phys.Lett.285 (1998) 170-173

[33] LF.Matta, R.J.Boyd, An Introduction of the Quantum theory of Atom in Molecule, Wiley-VCH Verlag Gmbh, 2007

[34] R. G. Parr, J. Am. Chem. Soc., 121 (1999) 1922-1924

[35] P. K. Chattaraj, S. Giri, J. Phys. Chem. A, 111 (2007) 11116

[36] P. K. Chattaraj, S. Giri, S. Duley, Chem. Rev., 111 (2011) PR43-PR75

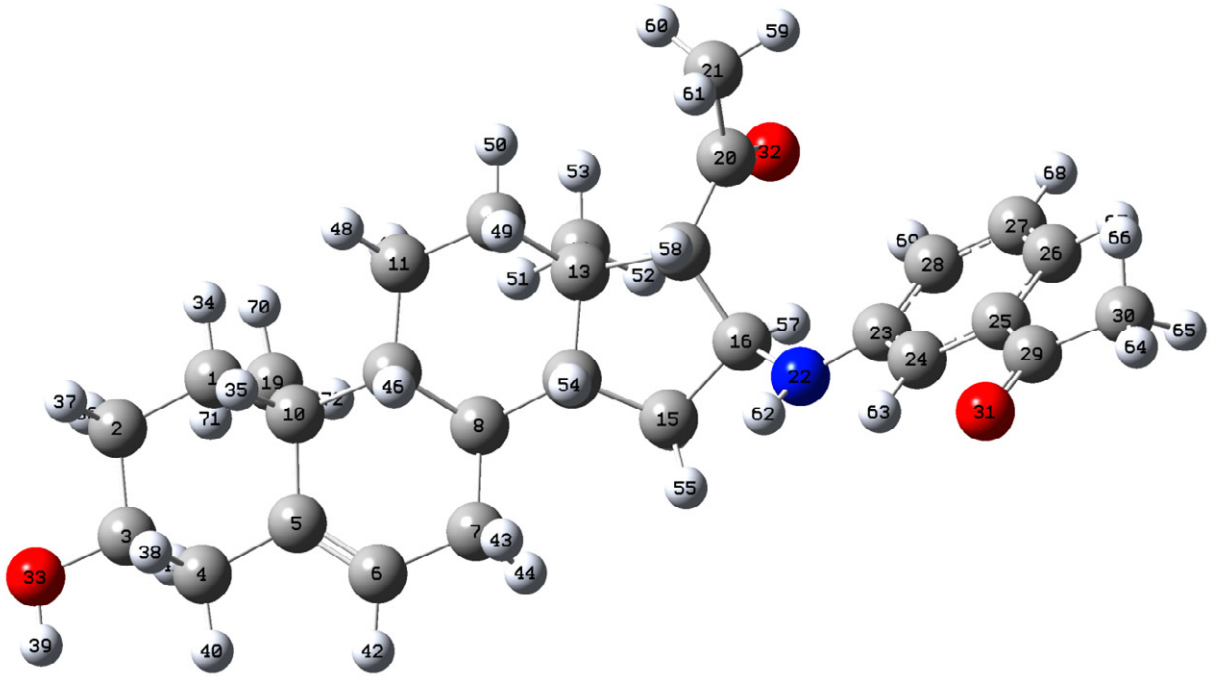

Fig.1. Optimized geometry of Compound **3** using B3LYP/6-31G(d,p) level of theory.

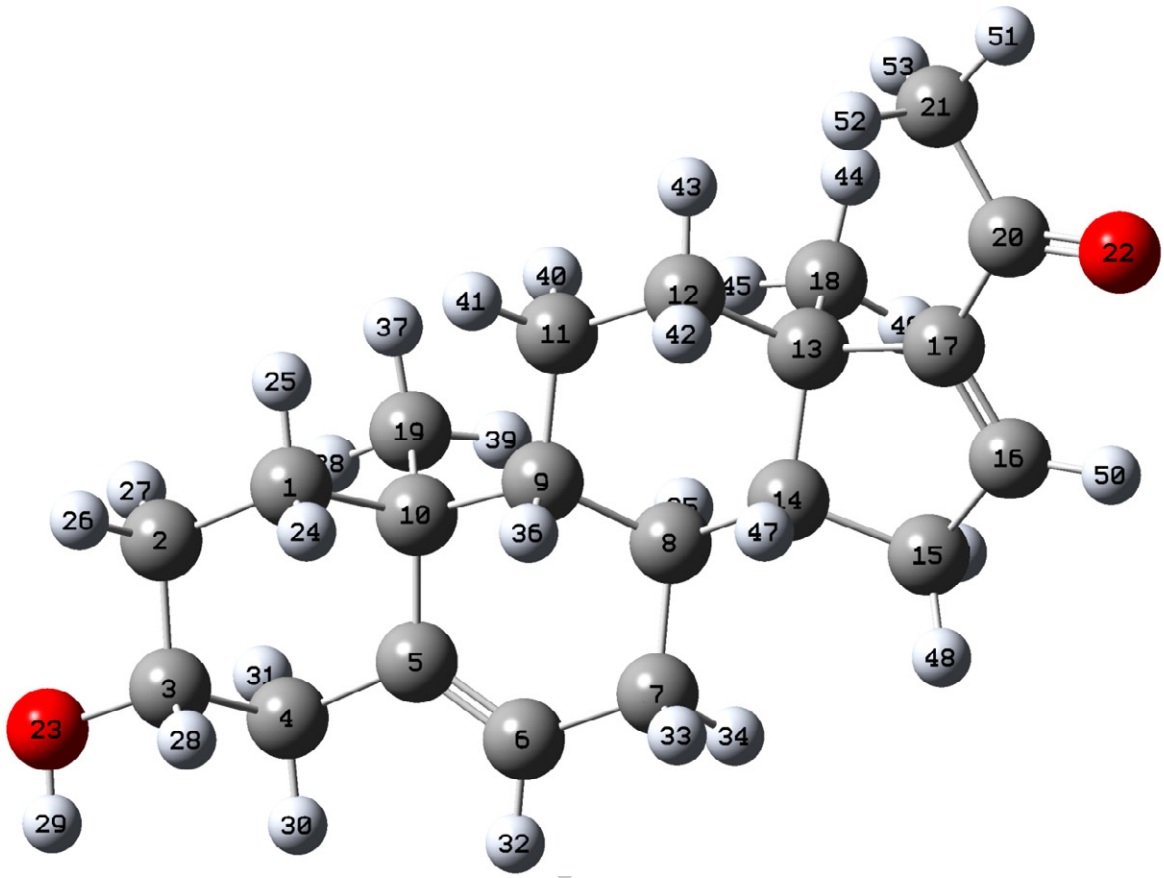

Fig. 2. Optimized geometry of Compound **1** using B3LYP/6-31G(d,p) level of theory.

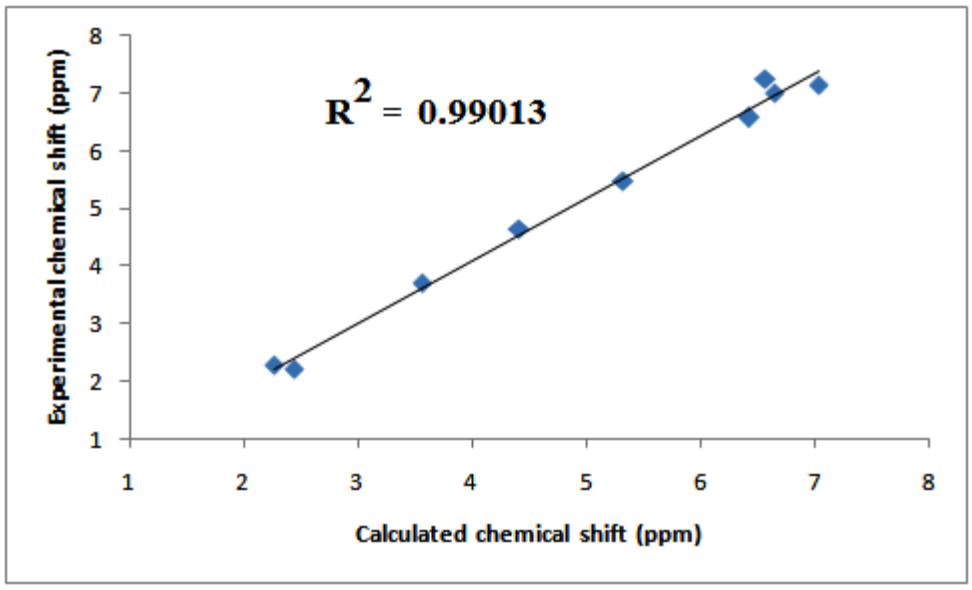

Fig. 3. Correlation graph between Experimental and Calculated ^{1}H NMR chemical shift of compound **3**.

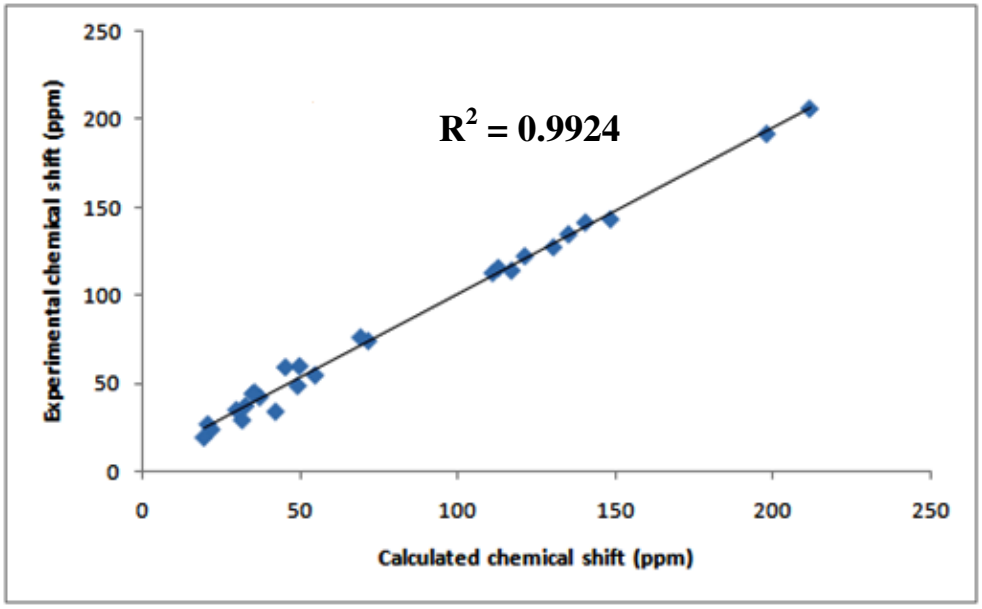

Fig. 4. Correlation graph between Experimental and Calculated ^{13}C NMR chemical shift of compound **3**.

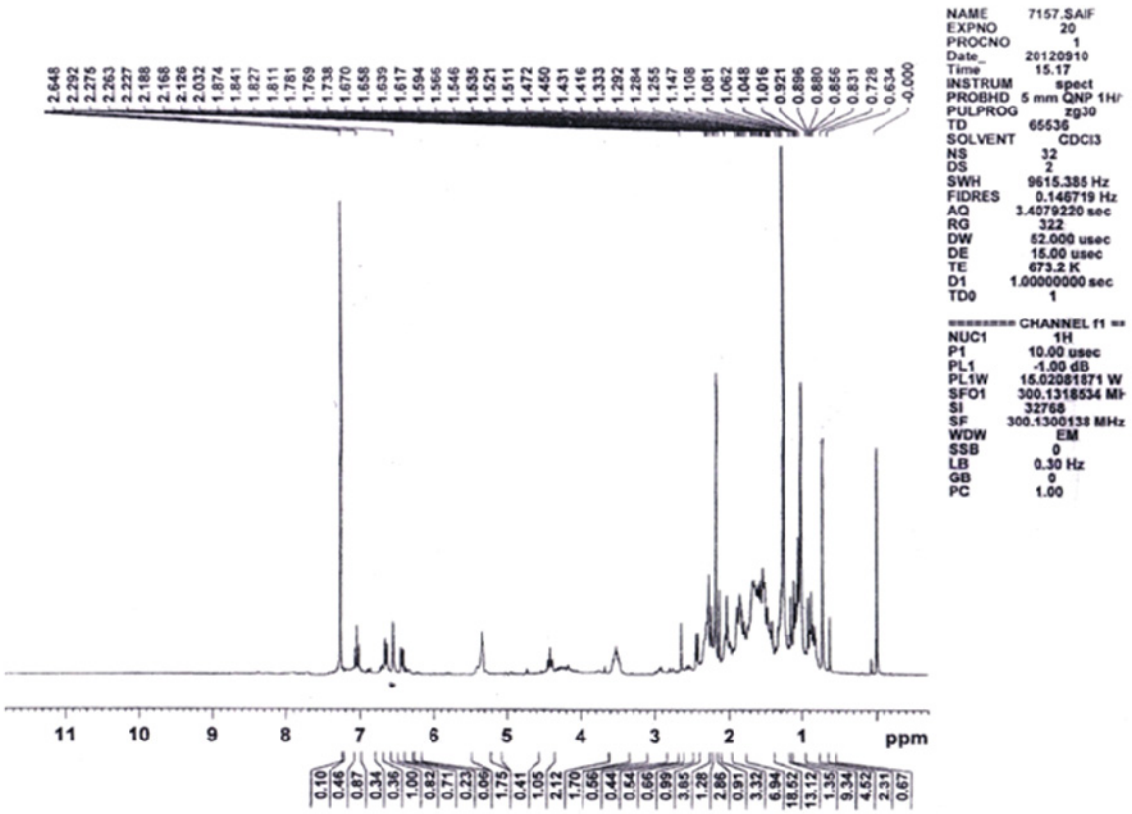

Fig. 5. ^{1}H NMR spectrum of compound **3**.

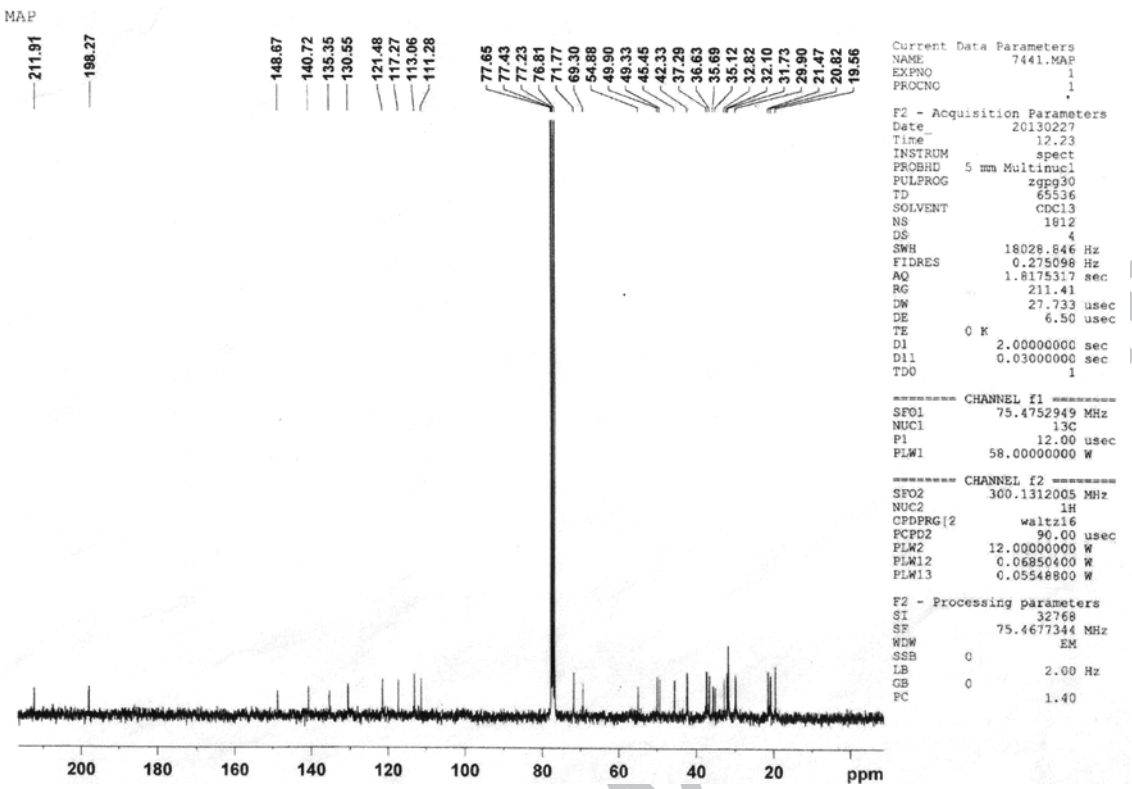

Fig. 6. ^{13}C NMR spectrum of compound **3**.

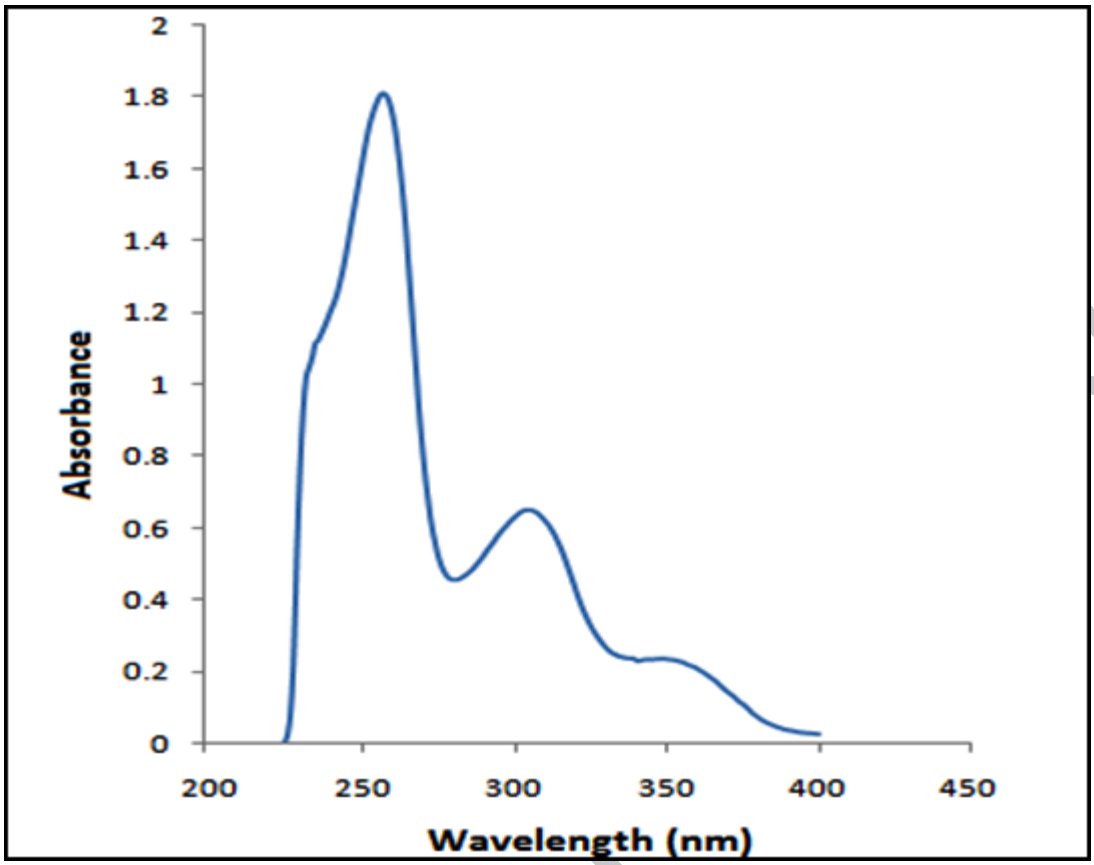

Fig.7. UV–Vis spectrum of compound **3**.

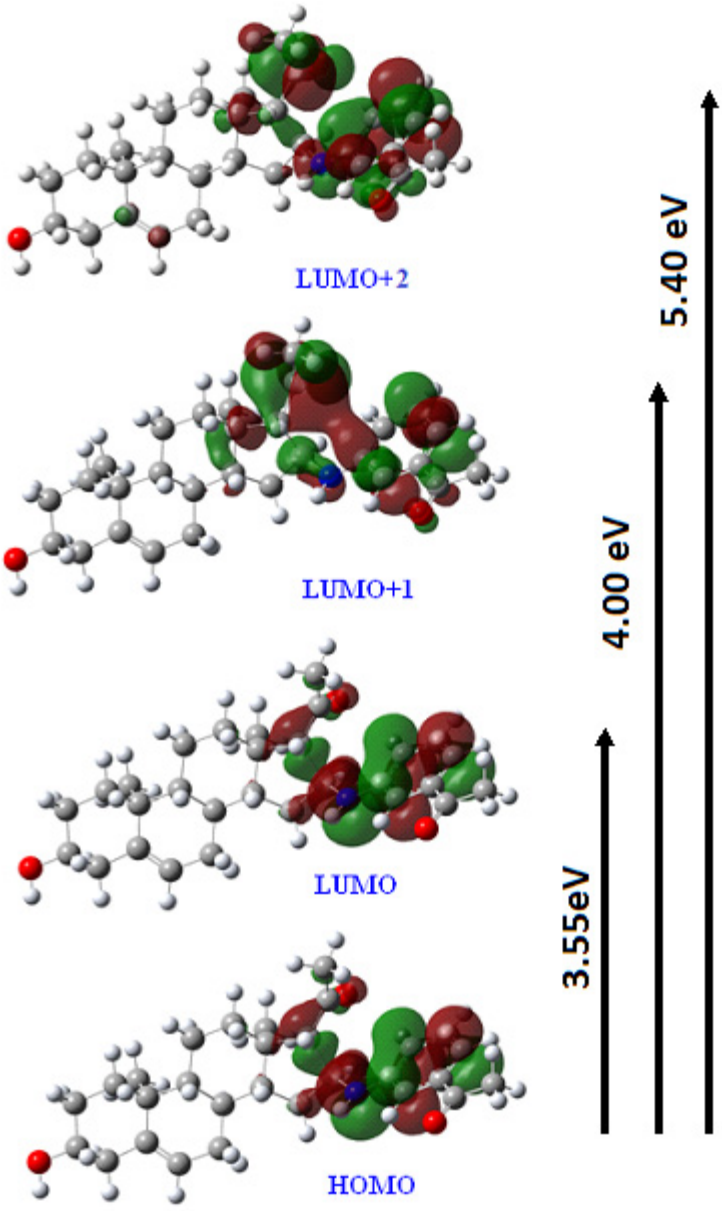

Fig. 8. Molecular orbitals (HOMO, LUMO, LUMO+1) of compound **3** at B3LYP/6-31G (d, p) level.

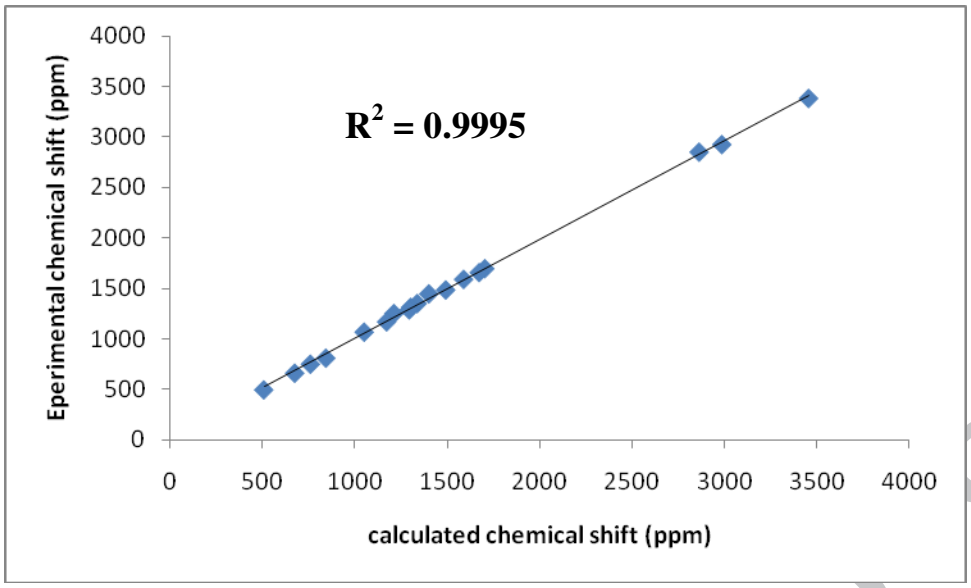

Fig. 9. Correlation graph between Experimental and Calculated IR wavenumbers of compound **3**.

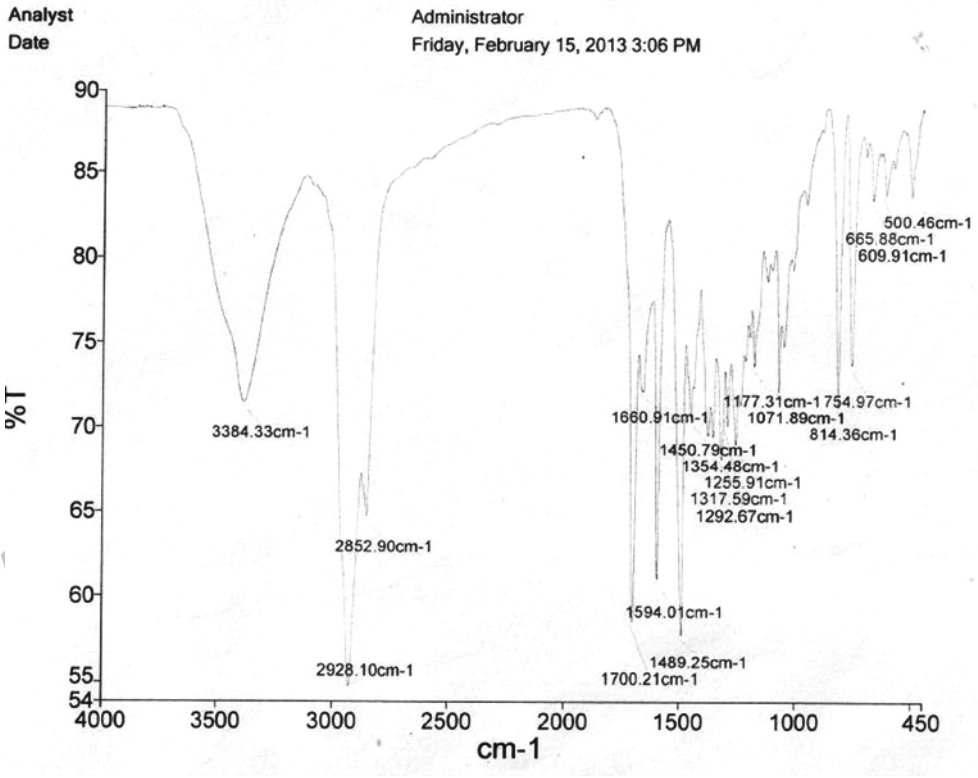

Fig. 10. IR spectrum of compound **3**.

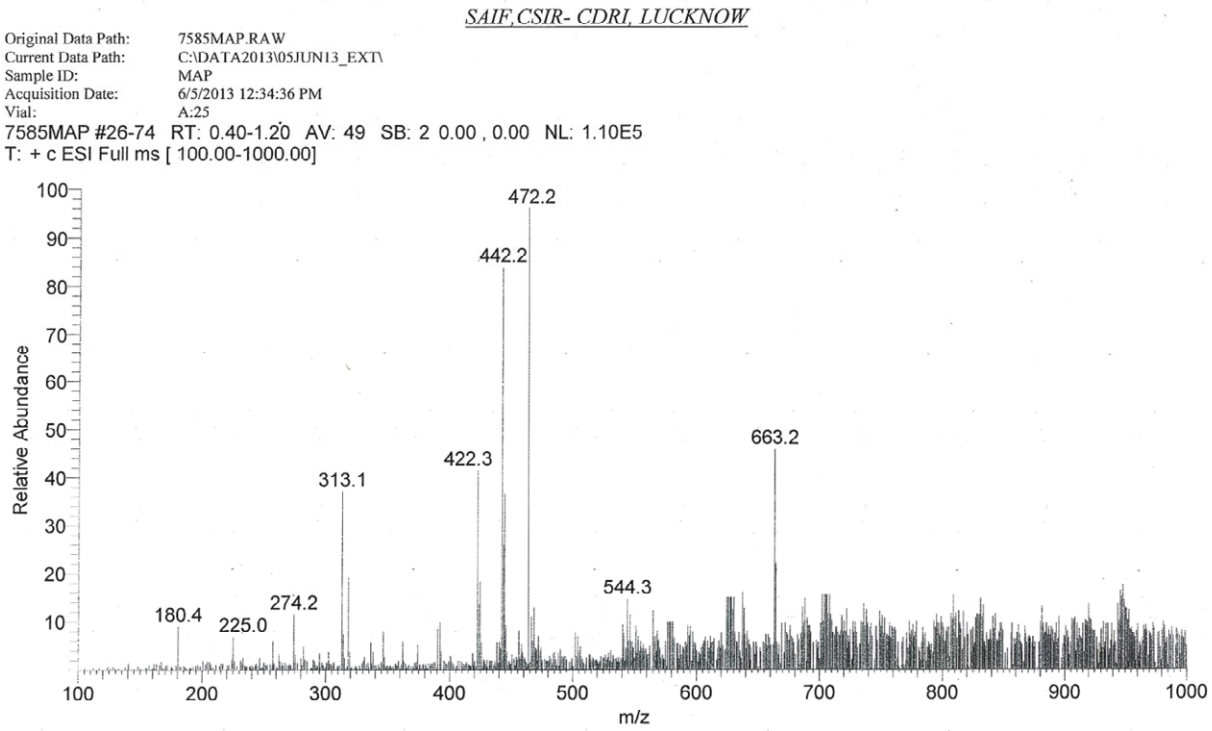

Fig. 11. Mass Spectrum of compound **3**.

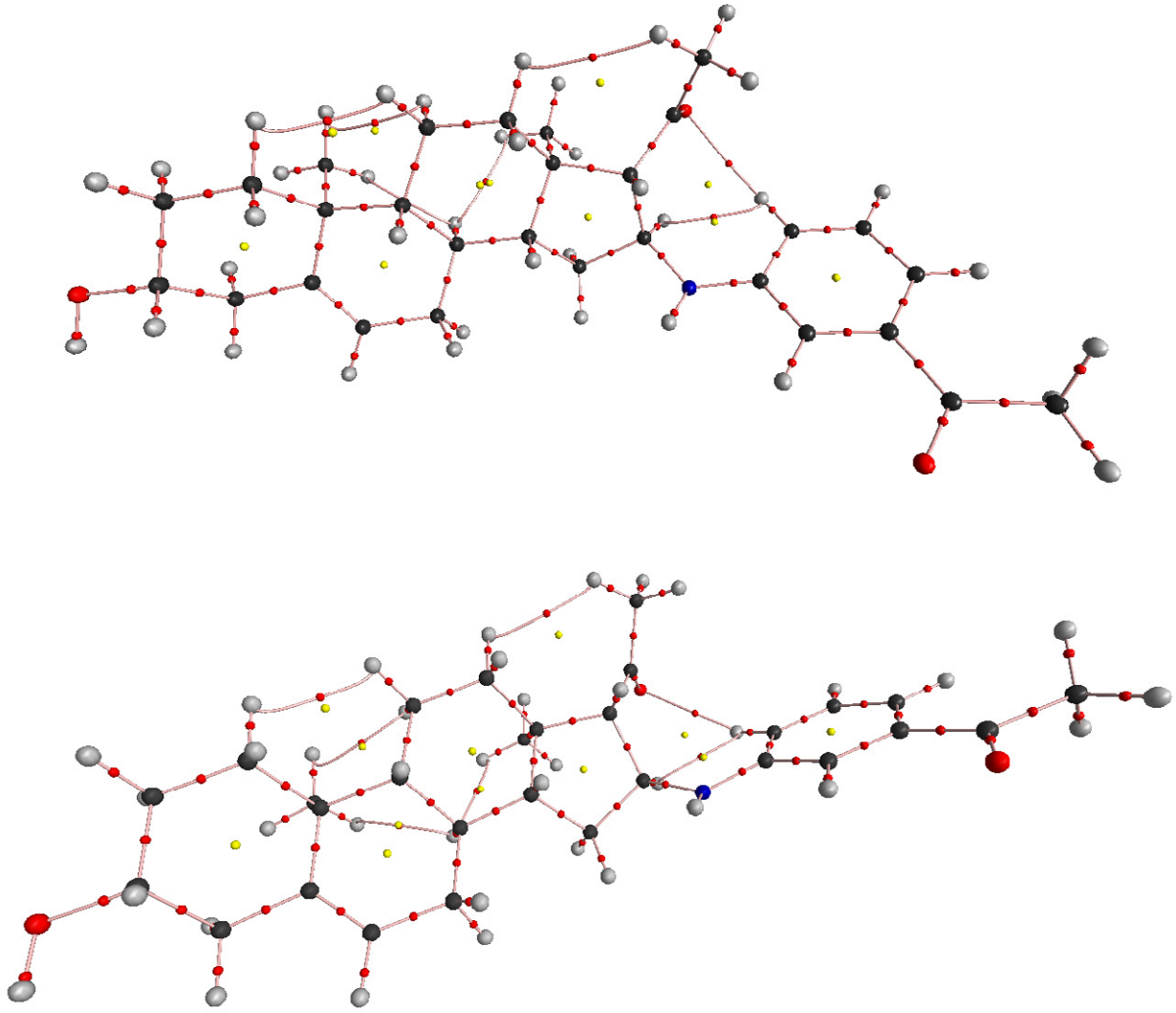

Fig. 12. Molecular graph of compound **3** at B3LYP/6-31G (d, p) level using AIM program: bond critical points (small red sphere), ring critical points (small yellow sphere) and bond path (pink lines).

Table 1
Comparison between optimized geometrical parameters for compound **1** and **3** using B3LYP/6-31G (d, p).

Compound 1		Compound 3	
Bond length(Å)		Bond length(Å)	
C16-C17	1.34	C16 –C17	1.57
C5-C6	1.33	C5-C6	1.33
C3-O23	1.42	C3-O33	1.44
C20-O22	1.22	C20-O32	1.22
C10-C19	1.55	C10-C19	1.55
C13-C18	1.55	C13-C18	1.54
C17-C20	1.49	C29-O31	1.42
C20-C21	1.51	C23-C24	1.40
C6-C7	1.50	C24-C25	1.39
C15-C16	1.50	C25-C26	1.40
C4-C5	1.51	C26-C27	1.39
C13-C17	1.54	C27-C28	1.39
		C28-C23	1.41
		C16-N22	1.45
		N22-C16	1.38
Bond angle(^{o})		Bond angle(^{o})	
O23-C3-C4	111.8	O33-C3-C4	111.8
C15-C16-C17	112.5	C15-C16-C17	105.4
C17-C20-O22	120.3	C15-C16-N22	110.0
C16-C17-C20	120.3	C16-N22-C23	125.2

C4-C5-C6	120.4	C17-C20-O32	121.4
O22-C3-C2	107.5	C25-C29-O31	120.9
Torsional angle(°)		Torsional angle(°)	
C1-C10-C5-C4	46.8	C1-C10-C5-C4	47.0
C19-C10-C5-C6	108.4	C19-C10-C5-C6	108.4
C7-C8-C9-C11	-60.7	C7-C8-C9-C11	-59.8
C14-C8-C9-C11	47.7	C14-C8-C9-C11	48.4
C12-C13-C14-C15	63.8	C12-C13-C14-C15	59.8
C17-C13-C14-C15	-35.6	C17-C13-C14-C15	-47.1
C13-C17-C20-O22	-178.3	C13-C17-C20-O32	-83.5

Table 2

The Comparison between experimental and theoretical ^{1}H and ^{13}C NMR chemical shifts δ (ppm) from TMS for compound **3**.

Atom no.	Experimental ^{1}H NMR	Calculated ^{1}H NMR	Atom no.	Experimental ^{13}C NMR	Calculated ^{13}C NMR
H68 (t)	7.03 (J= 7.8 Hz)	7.15	C20	211.91	206.32
H67 (d)	6.64 (J= 6.3 Hz)	7.02	C29	198.27	192.08
H63 (s)	6.56	7.25	C23	148.67	143.59
H69 (d)	6.42 (J= 6.3 Hz)	6.57	C5	140.72	141.72
H42 (d)	5.32 (J= 5.1 Hz)	5.48	C25	135.35	135.04
H57 (t)	4.41 (J= 7.5 Hz)	4.64	C27	130.55	127.70
H38 (m)	3.56	3.71	C6	121.48	122.60
H58(d)	2.44 (J= 6.0 Hz)	2.21	C28	117.27	114.42
H-64,65,66 (s)	2.26	2.29	C26	113.06	115.82
H -59,60,61 (s)	2.16	1.90	C24	111.28	113.06
H- 70,71,72 (s)	1.01	1.09	C3	71.77	74.50
H-51,52,53 (s)	0.72	0.79	C17	69.30	76.50
			C14	54.88	60.12
			C9	49.90	55.10
			C4	49.33	49.03
			C16	45.45	59.56

			C2	42.33	34.32
			C1	37.29	42.58
			C10	35.69	45.21
			C12	35.12	44.48
			C7	32.82	37.61
			C30 &C8	31.73	29.52
			C21	29.90	35.25
			C19	21.97	24.17
			C11	20.82	27.10
			C18	19.56	19.64

Table 3

Electronic transitions (calculated and experimental) for compound 3.

Compounds	Molecular orbitals	E (eV)	Calculated (λ_{max})	Assignments	Oscillatory strength *(f)*	Observed (λ_{max})
1.	H→ L	3.55	348	n → π*	0.0290	356
2.	H→L+1	4.00	309	n → π*	0.0447	304
3.	H→L+2	5.40	229	π → π*	0.4762	256

Table 4

Second order perturbation theory analysis of Fock Matrix in NBO Basis of compound **3**.

Donor (I)	Type of band	Occupancy	Acceptor (J)	Type of band	Occupancy	E2 (kJ/mol)[a]	E (j)-E(i) (a.u)[b]	F (i , j) (a.u)[c]
C23–C24	π	1.608	C28–C27	π*	0.3433	17.78	0.28	0.064
C28–C27	π	1.608	C24–C25	π*	0.4158	23.06	0.28	0.072
O32	π	1.689	C23–C24	π*	0.3835	20.31	0.28	0.069
O31	π	1.689	C26–C25	π*	0.4158	17.51	0.28	0.065
C25–C26	n	1.889	C20–C17	π*	0.0641	19.45	0.66	0.102
N22	n	1.891	C25–C29	π*	0.0663	19.45	0.69	0.105
C6-H42	n	1.891	C29–C30	π*	0.0522	20.12	0.64	0.103
C21-H61	π	1.646	C23–C24	π*	0.3835	18.32	0.28	0.064
C6-C7	π	1.646	C28–C27	π*	0.3433	22.20	0.28	0.070
C7-H43	π	1.646	C29–O31	π*	0.1304	18.20	0.27	0.066
C14-H54	n	1.780	C23–C24	π*	0.4158	34.27	0.29	0.093
C18-H51	π	1.978	C5-C10	π*	0.0372	6.84	0.91	0.071
C2-H37	π	1.967	O32-C20	π*	0.0972	6.34	0.53	0.052

C4-H40	σ	1.980	C5-C4	σ*	0.0234	4.13	1.04	0.059
C24-H63	σ	1.970	C6-C5	π *	0.0754	4.30	0.56	0.044
	σ	1.968	C13-C18	σ*	0.0242	3.88	0.85	0.051
	σ	1.987	C13-C17	σ*	0.0309	3.03	0.84	0.045
	σ	1.978	C10-C1	σ*	0.0286	3.72	0.84	0.050
	σ	1.980	C5-C10	σ*	0.0372	4.17	0.90	0.055
	σ	1.972	N22-C23	σ*	0.0252	3.64	1.16	
0.058								

[a] Energy of hyper conjugative interactions.
[b] Energy difference between donor and acceptor i and j NBO orbitals.
[c] Fock matrix element between i and j NBO orbitals.

Table 5

Experimental and calculated (selected) vibrational wavenumbers of monomer using B3LYP/6-31G (d,p) and their assignments for compound **3**.

	Wavenumber unscaled	Wavenumber scaled	Exp. Wavenumbers	Assignment
	3809	3660	3100-3610	Stretching vibration of H39O33

3597	3456	3384.33	Stretching vibration of N22H62
3109	2987	2928.10	Stretching vibration of Me21
2981	2864	2852.90	Stretching vibration of CH_2
1774	1705	1700.21	Stretching vibration of C(29)=O(31)
1742	1674	1660.91	Stretching vibration of C(5)=C(6)
1655	1590	1594.01	Stretching vibration of aromatic C=C
1554	1493	1489.25	N-H bending for secondary amine
1459	1402	1450.79	C=C ring stretching of aromatic
1394	1339	1354.48	Deformation of CH_3-30
1357	1304	1317.59	C-N(N22-C23) stretching of secondary amine
1341	1289	1292.67	CH_2 wagging and twisting
1263	1213	1255.91	C-N(C16-N22) stretching of secondary amine
1095	1052	1071.89	C-O(C3-O39) stretching
879.3	844.9	814.36	N22-H62 wagging
792.2	761.2	754.97	Aromatic C=C-H out of plane bending

	704.3	676.7	665.88	Aromatic C=C-H out of plane bending

Table 6

Geometrical parameters (bond length) and topological parameters for bonds of interacting atoms: electron density (ρ_{BCP}), Laplacian of electron density ($\nabla^2\rho$(BCP)), electron kinetic energy density (G_{BCP}), electron potential energy density (V_{BCP}), total electron energy density (H_{BCP}) at bond critical point (BCP) and estimated interaction energy (E_{int}) of compound **3**.

Interaction	Bond length	$\rho_{(BCP)}$	$\nabla^2\rho_{(BCP)}$	G_{BCP}	V_{BCP}	H_{BCP}	E_{int}

H70		0	0.04	0	-0	0	-1
…..H	2.	.	4	.	.	.	.
47	17	010	0.038	008	0.006	002	88
H34		0	0.032	0	-0	0	-0
…..H	2.	0	0.037	.	.	.	.
48	19	.	0.017	007	0.002	005	62
H72		009	0.040	0	-0	0	-1
…..H	2.	0	0.030	.	.	.	.
45	25	.		006	0.004	002	25
H45		008		0	-0	0	-1
…..H	2.	0		.	.	.	.
51	21	.		007	0.004	003	25
H50		009		0	-0	0	-0
…..H	2.	0		.	.	.	.
60	46	.		003	0.004	001	62
H57		004		0	-0	0	-1
…..H	2.	0		.	.	.	.
69	16	.		000	0.006	000	00
O32		004		0	-0	0	-1
…..H	2.	0		.	.	.	.
69	5	.		000	0.000	000	00

	2	0.0928	0.0806	-0.0025	0.0301	5.6-1.556

$\rho_{(BCP)}$, $\nabla^2\rho_{(BCP)}$, G_{BCP}, V_{BCP}, H_{BCP} (in a.u.); E_{int} (kcal/mol).

Table 7

Selected eletrophilic reactivity descriptors (f_k^+, s_k^+, ω_k^+) and nucleophilic reactivity descriptors (f_k^-, s_k^-, ω_k^-) of compound **1** and compound **3** using Hirshfeld atomic charge.

Atom no.	f_k^+	f_k^-	s_k^+	s_k^-	ω_k^+	ω_k^-
Compound 1						
C17	0.0712	0.0179	0.0140	0.0035	0.2013	0.0506
C16	0.1831	0.0513	0.0361	0.0101	0.5177	0.1450
Compo						

und 3						
C17	0.0 099	0.0 157	0.0 019	0.0 031	0.0 303	0.0 483
C16	0.0 082	0.0 233	0.0 016	0.0 046	0.0 253	0.0 717

GRAFICAL ABSTRACT:

Compound 16α-(3-acetyl phenyl amino)-3β- hydroxy pregn-5-ene-20-one was characterized with the aid of ^{1}H, ^{13}C-NMR, IR, UV and Mass spectrometry. Theoretical calculations were carried out with DFT, NBO analysis and AIM approach.

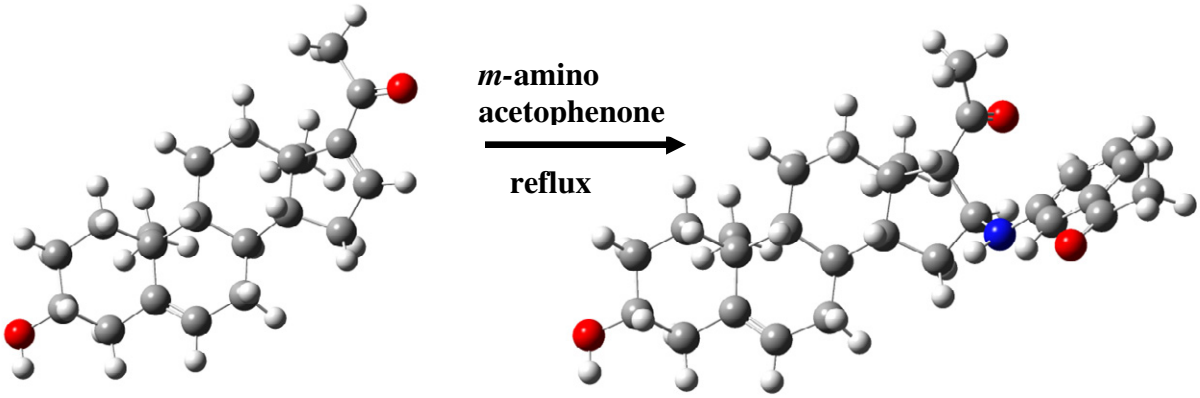

Highlights

- Compound **3** synthesized by Michael addition.
- Compound **3** characterized with the help of ^{1}H, ^{13}C-NMR, IR, UV and ESI-MS.
- The experimental ^{1}H, ^{13}C NMR and IR values correlated with calculated values.
- The $\pi \rightarrow \pi^*$, $\sigma \rightarrow \sigma^*$ and $n \rightarrow \pi^*$ interactions analyzed by NBO analysis.
- Weak intramolecular interactions and ellipticity analyzed by AIM approach.